ACS Catalysis

Letter

pubs.acs.org/acscatalysis

Steering the Chemistry of Carbon Oxides on a NiCu Catalyst

Erik Vesselli,*[,†,‡] Enrico Monachino,[†] Michele Rizzi,[§,⊥] Sara Furlan,[§,#] Xiangmei Duan,[#] Carlo Dri,[†,‡] Angelo Peronio,[†,‡] Cristina Africh,[‡] Paolo Lacovig,[∥] Alfonso Baldereschi,[§,⊥,×] Giovanni Comelli,[†,‡] and Maria Peressi[§,¶]

[†]Physics Department and CENMAT, University of Trieste, via Valerio 2, I-34127 Trieste, Italy

[‡]IOM-CNR Laboratorio TASC, Area Science Park, S.S. 14 km 163.5, I-34149 Basovizza (Trieste), Italy

[§]Physics Department, University of Trieste, Strada Costiera 11, I-34151 Trieste, Italy

[⊥]Institute of Theoretical Physics, École Polytechnique Fédérale de Lausanne (EPFL), CH-1015 Lausanne, Switzerland

[#]Department of Physics, Ningbo University, 818 Fenghua Road, Jiangbei District, 315211 Ningbo, People's Republic of China

[∥]Elettra-Sincrotrone Trieste S.C.p.A., Area Science Park, S.S. 14 km 163.5, I-34149 Trieste, Italy

[×]IOM-CNR DEMOCRITOS, Trieste, Italy

[¶]IOM-CNR DEMOCRITOS, Theory@Elettra Group, Trieste, Italy and Italian Consortium on Materials Science and Technology (INSTM)

Supporting Information

ABSTRACT: In the perspective of a sustainable energy economy, CO_2 reduction is attracting increasing attention as a key step toward the synthesis of fuels and valuable chemicals. A possible strategy to develop novel conversion catalysts consists in mimicking reaction centers available in nature, such as those in enzymes in which Fe, Ni, and Cu play a major role as active metals. In this respect, NiCu shows peculiar activity for both water-gas shift and methanol synthesis reactions. The identification of useful descriptors to engineer and tune the reactivity of a surface in the desired way is one of the main objectives of the science of catalysis, with evident applicative interest, as in this case. To this purpose, a crucial issue is the determination of the relevant active sites and rate-limiting steps. We show here that this approach can be exploited to design and tailor the catalytic activity and selectivity of a NiCu surface.

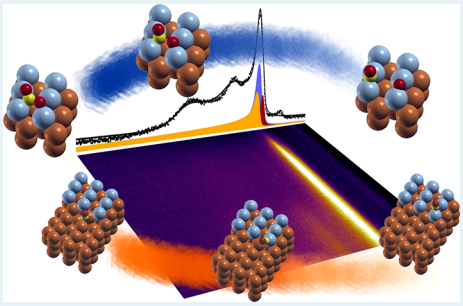

KEYWORDS: *nickel, copper, carbon dioxide, carbon monoxide, catalysis*

Achieving control of bond formation and dissociation in surface reactions is a key to making the chemistry of heterogeneous catalysis more energy-efficient and product-specific.[1,2] A linear scaling relationship (Brønsted–Evans–Polanyi, BEP) between adsorption and transition-state energies has often been observed in model cases and was proposed as a theoretical tool to describe or predict a catalyst's activity,[2] also in the case of Ni–Cu bimetallic surfaces.[3] It was recently shown that self-diffusion and segregation processes governed not only by energetics but also by kinetics, together with adsorbates coverage effects, can also play an important role.[4,5] Furthermore, the surface composition is influenced by the adsorbate–metal bond strength and by the chemical potential of the gas phase species.[6,7] Effective tuning of the bonds of reactants and intermediates with the surface would actually allow for simple engineering of a catalyst. This is a particularly hot topic in CO_2 (electro)reduction chemistry at Cu-based catalysts and electrodes.[8,9] On pure Ni, CO_2 reduction has recently been investigated down to the single-atom level, unveiling reaction mechanisms involving bent, activated CO_2 species,[10,11] formate as a stable spectator,[12] and hydrocarboxyl active species.[10−14] Within this complex framework, we show that the reduction rates of the activated CO_2 precursor and the adsorption energies and sites of the ad-species can be effectively controlled by choosing proper Ni doping of a Cu model catalyst surface. The Ni surface concentration accounts for effects previously observed under standard reaction conditions on model catalysts.

We performed temperature programmed desorption (TPD) experiments following adsorption of CO_2 at liquid nitrogen (LN_2) temperature under ultrahigh vacuum (UHV) conditions on a Ni film grown on a Cu(110) surface. Both desorption and decomposition take place upon heating, yielding straightforward information about the desorption energies of carbon dioxide and carbon monoxide, together with the carbon dioxide conversion efficiency, as a function of the Ni coverage (1 ML corresponds to one adsorbed atom/molecule per surface unit cell, 1.09×10^{15} atoms/cm^2). The CO_2 conversion efficiency, as

Received: May 3, 2013
Revised: June 4, 2013
Published: June 6, 2013

   dx.doi.org/10.1021/cs400327y | ACS Catal. 2013, 3, 1555−1559

obtained from the TPD data after exposure of the clean surface to gas phase CO_2, is defined as the ratio $\theta_{CO}/(\theta_{CO}+\theta_{CO2})$. The Ni film was grown on the Cu(110) surface by chemical vapor deposition following a recipe that guarantees minimal Ni/Cu intermixing in the temperature ranges used in our experiments.[4]

In panel a of Figure 1 it can be observed that the thickness of the Ni film affects both the saturation coverage of chemisorbed

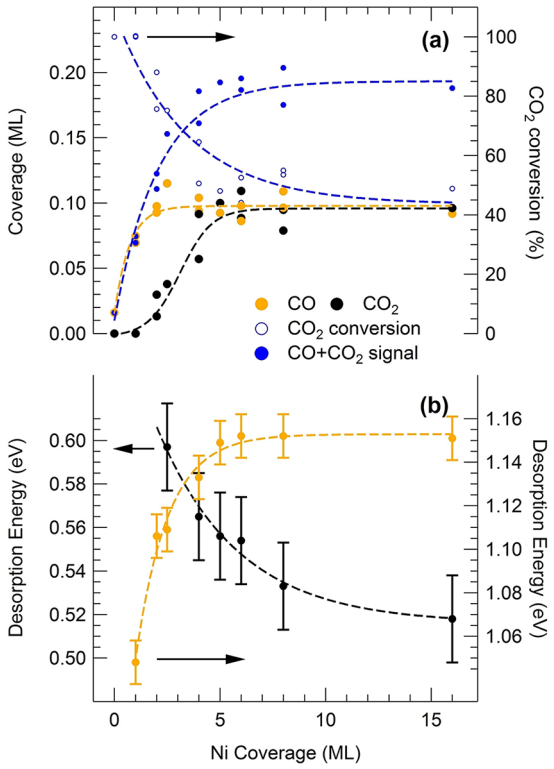

Figure 1. Tuning the catalyst activity as a function of Ni coverage. (a) Carbon dioxide reactivity: total coverage (blue markers), direct desorption vs decomposition (black and orange markers, respectively), and conversion rate (empty circles). (b) Carbon dioxide vs carbon monoxide desorption energies. Desorption energy and adsorbates coverage values are obtained from temperature-programmed desorption experiments. Lines are drawn to guide the eye.

CO_2 and its dissociation/desorption ratio, yielding conversion efficiencies from 100% to 50%. As for pure Ni(110),[11] we find that competition between CO_2 desorption and decomposition takes place in the 200−250 K temperature range, where mechanisms governing Ni diffusion and segregation from ad-islands are still inactive.[4] Conversely, on pure Cu, only CO_2 physisorption occurs, yielding no decomposition under UHV conditions.[15]

The CO_2 and CO desorption energies were extracted from the TPD spectra and are shown as a function of the Ni coverage in panel b of Figure 1. Remarkably, a very different behavior is observed: for increasing Ni thicknesses, CO is progressively stabilized, in agreement with previous reports.[16] The same trend is observed for both CO deposited from the gas phase and for CO obtained from the decomposition of CO_2, both for saturation and small CO coverage (not shown here). Concerning CO_2, we find that Ni doping stabilizes a chemisorbed state, whose binding energy decreases for thicker Ni films, at variance with what is observed for CO. This indicates that the concentration of Ni at the surface is an appropriate and easily accessible parameter to tune the reactant and product adsorption energies, thus moving the decomposition/desorption ratio along the observed conversion efficiency curve of panel a. This result provides a simple explanation of the behavior observed for the CO_2 reduction to methanol on Ni/Cu(100) under high pressure conditions,[6,7] where Ni doping yields a higher turnover frequency. It was suggested that the reaction occurs at Ni sites, tentatively ascribing the effect to a CO-promoted surface segregation of Ni at the reaction temperatures employed in the experiments and to the interplay between the formation of CO_2−Ni and CO-Ni bonds. We directly confirm this hypothesis.

To provide an atomic scale interpretation of our data, we performed an extensive set of density functional theory (DFT) ab initio calculations. The main energy values obtained are listed in Table 1 and represented in Figures 2 and 3. The most

Table 1. DFT-GGA Energies (in eV) for Molecules and Atoms Relevant to the Present Study at a Coverage of θ = 1/6 ML[a]

	E_{ads} (CO_2)	E_{ads} (CO + O)	ΔE_{diss} (CO_2)	E_{ads} (CO)		E_{ads} (O)
config	best adsorption site			short bridge	on-top	pseudo-3-fold
Cu	−0.23[b]	+0.62	1.18	−1.04	−1.02	−1.66
1 ML Ni/Cu	−1.00	−1.66[c]	0.26	−2.41	−1.96	−2.51[c]
Ni	−0.70	−1.19	0.50	−2.10	−1.90	−2.29

[a]Values in the left part of the table are referred to gas phase CO_2; those for CO and O separately are related to the corresponding gas phase molecule. E_{ads} is the adsorption energy; ΔE_{diss} is the dissociation barrier. If not otherwise specified, the best adsorption site is hollow-up for CO_2 and SB for CO. [b]Physisorbed configuration. [c]SB site for O.

relevant aspects are the following: Ni doping of Cu both lowers the CO_2 dissociation energy barrier and stabilizes the reactant and products with respect to the pure metal surfaces (Figure 2, panel a). In the case of pure Cu (orange curve) CO_2 physisorption, occurring below 100 K,[15] is energetically even more convenient than adsorption of the CO + O products. For the doped surface (1 ML Ni, dashed curve), dissociation of chemisorbed CO_2 is strongly favored with respect to desorption (corresponding to the zero of the energy scale, indicated by the horizontal black dashed line), but for pure Ni (blue curve), the two processes compete. The DFT results thus account for the decomposition/desorption ratio trend obtained by TPD (Figure 1, panel a). Furthermore, by plotting our calculated energies and literature values for other surface orientations (Figure 2, panel b), we find that the BEP[2] relationship holds also for CO_2 decomposition.

In Figure 3, calculated adsorption energies of individual species are compared. We find that 1 ML Ni/Cu(110) provides for CO_2 a strong overbinding with respect to pure Ni or Cu substrates (black line). Even a single substitutional Ni surface atom leads to strengthening of the molecule−Ni bond. The DFT calculations explain therefore our observations for CO_2. Theory predicts an overbinding effect also in the case of CO at low coverage (θ = 1/6 ML) for adsorption at both bridge and on-top sites (dotted and dashed orange lines in Figure 3, respectively). This result is apparently in contrast with the measured CO desorption energy that shows, indeed, a monotone behavior as a function of the Ni coverage, rather than an overbinding at 1 ML. This puzzling point can be explained considering a site change for CO from on-top to

dx.doi.org/10.1021/cs400327y | ACS Catal. 2013, 3, 1555−1559

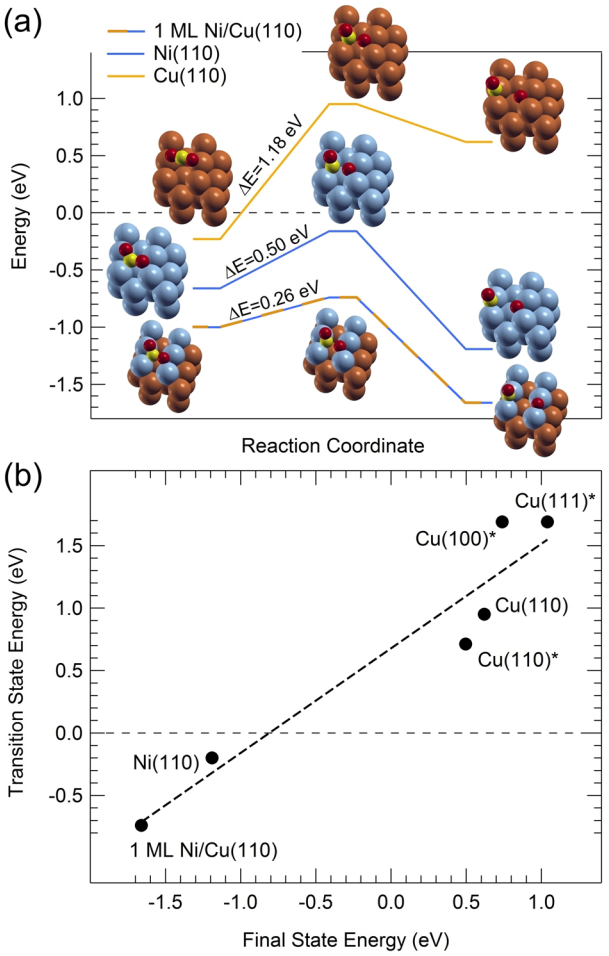

Figure 2. Cleavage of the O−CO bond in adsorbed carbon dioxide at mono- and bimetallic NiCu surfaces clearly shows that Ni doping promotes decomposition. (a) Path for decomposition on Cu(110) (orange), Ni(110) (blue), and 1 ML Ni/Cu(110) (dashed). Ball models of the corresponding initial, transition, and final states as obtained from DFT calculations are also shown. All energies are referred to gas phase CO_2. Atom color legend: Cu (orange), Ni (blue), oxygen (red), carbon (yellow). (b) The BEP relationship holds for CO_2 dissociation into CO + O. An asterisk (*) indicates values from the literature.[23−25]

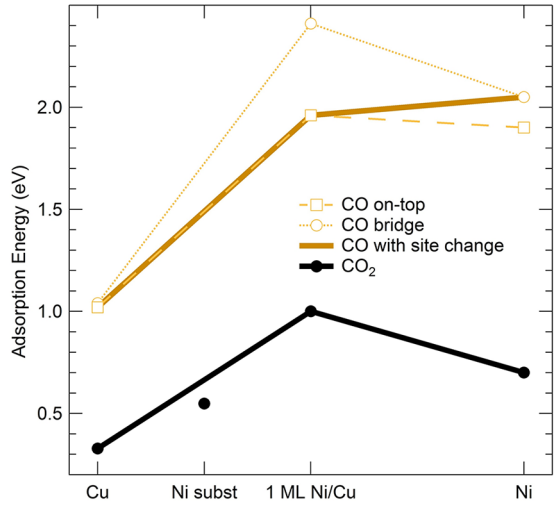

Figure 3. Calculated adsorption energies for CO and CO_2. Within the DFT framework, a remarkable overbinding is found for CO_2 adsorbed on 1 ML Ni/Cu(110) with respect to bare Cu or Ni terminations (black). CO adsorption in bridge and on-top sites at a coverage of θ = 1/6 ML shows a similar behavior (dotted and dashed orange lines, respectively). The experimental monotone trend for the binding energy of CO is recovered when considering the on-top/bridge site change (orange continuous line). The absolute value of the adsorption energy is reported.

short bridge (SB) for increasing Ni coverage. From the on-top site on Cu (as found experimentally and reported in the Supporting Information, and energetically equivalent to SB in our calculations), CO has to change to SB, which is the most stable on the Ni(110) surface. If we consider that such a change occurs at 1 ML Ni/Cu(110), we then obtain the orange continuous line in Figure 3, thus reproducing the experimentally observed monotone trend for CO reported in panel b of Figure 1.

We further investigated the CO site change mechanism by means of time-resolved photoelectron spectroscopy uptake and desorption experiments at higher coverage. In a nutshell, we found that the adsorption of CO at NiCu surfaces is a complex phenomenon, determined by diffusion, site change mechanisms, and lateral interactions. We exploited synchrotron radiation high-energy resolution, time-resolved, core level X-ray photoelectron spectroscopy (XPS)[17] to follow the evolution of the Ni, Cu, C, and O core levels during both CO uptake and desorption from the Ni/Cu(110) surface under UHV. After desorption of CO, the Ni and Cu 3p signals recover to the intensity of the bare Ni/Cu sample, thus confirming, in agreement with our previous findings,[4] that there is no observable dilution of the metallic film into the bulk in the temperature range in which CO is stable at the surface. From the C and O 1s core level shifts, monitored upon CO adsorption and desorption for different Ni surface coverage values, three nonequivalent CO adsorbed species could be unambiguously identified in the complex XPS spectra. Selected core level spectra of the CO/Ni/Cu(110) system are reported and discussed in the Supporting Information. We could identify C and O 1s components originating from CO molecules adsorbed at on-top Cu sites (285.9 and 532.8 eV), at on-top Ni sites (285.8 and 532.4 eV), and at short-bridge Ni sites (285.4 and 531.0 eV).

Figure 4 reports the local coverage extracted from the intensity evolution of the O 1s core level components at a selected Ni surface coverage of 0.46 ML. Four panels are present in the figure: a and c show the uptake curves, obtained upon CO adsorption at LN_2 temperature; b and d report the CO evolution during a subsequent annealing. Each panel is divided in two by a horizontal dotted line, separating complementary data. In panels a and b, the CO coverage at Cu (upper part) and at Ni (lower part) ad-islands is reported symmetrically. From the data in panel a, a striking difference in the adsorption curves is apparent, with different concavity for Cu and Ni. Since CO can easily diffuse at LN_2 temperature on both Ni and Cu, due to the low hopping barrier,[18] the observed profiles indicate that CO impinging at Cu sites migrates to the Ni ad-islands. We independently confirmed this migration with simulations based on molecular dynamics methods (see Supporting Information). Indeed, using a simple model that assumes CO diffusion from Cu to Ni sites to be proportional to the number of occupied and free sites, respectively, at the island perimeters, we obtained the black dashed lines in panel a of Figure 4, reproducing the trends observed in the experimental

dx.doi.org/10.1021/cs400327y | ACS Catal. 2013, 3, 1555−1559

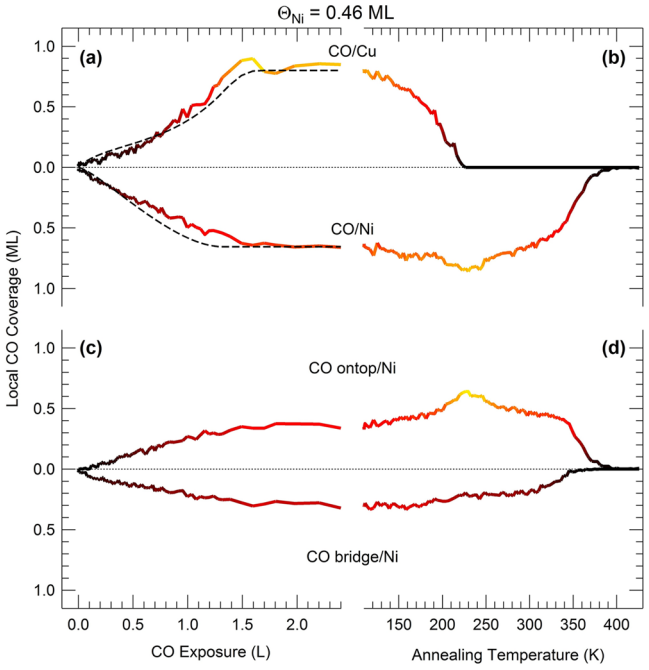

Figure 4. Tuning adsorption, diffusion, and desorption processes for carbon monoxide. From time-resolved in situ photoelectron spectroscopy of the C and O 1s core levels, the exposure and temperature dependence of the CO population of Ni vs Cu, and Ni-on-top vs Ni-bridge sites has been unveiled, proving the role of diffusion and site-change mechanisms. The black dashed lines correspond to the best fit of the data according to a simple adsorption/diffusion model. Ni coverage corresponding to shown data: 0.46 ML.

data. Upon heating, CO from Cu both desorbs and migrates to Ni where the local CO coverage increases with temperature (Figure 4, panel b), reaching a maximum at 225 K, corresponding to densely packed CO/Ni islands. Panels c and d show detailed information about CO adsorption inside the Ni ad-islands, distinguishing between on-top and bridge sites (upper and bottom parts of the panels, respectively). From the data in panel d, we can see that although CO migrates from Cu populating on-top Ni sites, a parallel CO site change process (bridge to on-top) occurs within the Ni islands. The annealing process therefore introduces a strong asymmetry in the relative population of Ni sites, which were instead equally occupied at the end of the uptake (panel c). Actually, our XPS data reveal a complex picture: by increasing the temperature, the local CO coverage on Ni increases and the relative population of on-top and bridge sites changes, and desorption occurs from the former sites, at variance with the pure Ni(110) surface.[11] For a Ni film thickness >1 ML, bridge sites already dominate instead (see Supporting Information). Calculations performed for progressive desorption of CO from densely packed adsorbed configurations (θ=0.75 ML) on pure Cu, pure Ni, and 1 ML Ni/Cu (110) surfaces indicate the presence of a strong lateral repulsion between the adsorbed CO molecules, particularly strong for 1 ML Ni/Cu system. This repulsion acts in the same direction of the site change considered in the low CO coverage regime, suppressing the overbinding with the surface and therefore yielding a monotonic growing trend of the CO adsorption energy for increasing Ni coverage.

In summary, we have identified a potential tool for driving surface activity and selectivity for CO_2 conversion, with a strong impact on the CO_2 reduction efficiency. Using a combined experimental and theoretical approach, we have, indeed, shown that at the Ni/Cu catalyst surface the local Ni coverage is strictly connected not only to adsorption, but also to diffusion, site-change, and local coverage of the adspecies. Our findings provide a clear explanation for the enhanced reactivity observed on a similar system toward CO_2 conversion to methanol under realistic conditions.[6] The proposed tool is relevant also in the case of CO reduction to methanol, providing the capability of tuning not only the conversion rate but also the selectivity.[19]

A direct transferability of the results obtained under UHV at low temperatures to realistic reaction conditions is not straightforward and requires pressure, temperature, and material gap issues to be considered. Concerning the material gap, experimental observations at high pressure on Ni-doped Cu single crystals have already shown an enhanced CO_2 conversion efficiency that was ascribed to the reactivity of Ni sites.[6,7,20] The latter significantly lower the barrier for the initial CO_2 hydrogenation steps with respect to the pure Cu termination,[6] in agreement with UHV studies,[12,13] whereas Cu sites yield methanol formation, avoiding complete C−O cleavage and production of methane, which actually occurs at pure Ni surfaces.[14] With respect to the pressure gap, further investigation in this direction with the aid of innovative in situ techniques such as high-pressure core-level photoelectron spectroscopy[21] and sum-frequency generation spectroscopy,[22] are needed to provide additional insight into the electronic configuration and the vibrational modes of surface intermediate species up to ambient pressures. Higher reaction temperatures can also be explored in this way, since a detectable surface concentration of the ad-species can be achieved. The chemical potential related to the gas phase, together with the higher available kinetic energy, may provide accessibility to parallel reaction routes. Within the framework of a sustainable energy economy based on renewable sources and on the recycling of pollutants, technologies related to the conversion of carbon dioxide into fuels and chemicals are of particular relevance. As discussed, NiCu alloys are showing interesting properties in the (electro)catalytic conversion of CO_2, and in the present report, we addressed and explained novel fundamental mechanisms that may guide the design of novel materials.

■ ASSOCIATED CONTENT

Supporting Information

Experimental methods and computational details, analysis of the C and O 1s core levels, molecular dynamics of carbon monoxide and dioxide on the NiCu alloy surface, kinetic model of the CO uptake, relative population of on-top and bridge sites. This material is available free of charge via the Internet at http://pubs.acs.org.

■ AUTHOR INFORMATION

Corresponding Author

*E-mail: (E.V.) vesselli@iom.cnr.it.

Notes

The authors declare no competing financial interest.

■ ACKNOWLEDGMENTS

The work was supported by the Italian MIUR through the project Futuro in Ricerca FIRB 2010 No. RBFR10J4H7. E.V. also acknowledges financial support from Fondazione Kathleen Foreman Casali, Beneficentia Stiftung, and Consorzio per l'Incremento degli Studi e delle Ricerche dei Dipartimenti di

Fisica dell'Università degli Studi di Trieste. E.V., C.D., and G.C. acknowledge support from Università degli Studi di Trieste through the project FRA 2012. C.A. and C.D. acknowledge support from Italian MIUR through projects PRIN 2010-2011 No. 2010N3T9M4 and Futuro in Ricerca FIRB 2010 No. RBFR10FQBL, respectively. Computational resources have been obtained in part through Italian SuperComputing Resource Allocation (ISCRA) grants of the Consorzio Interuniversitario CINECA, partly within the agreement between the University of Trieste and CINECA and partly under the HPC-EUROPA2 project (Project No. 583) with the support of the European Commission Capacities Area − Research Infrastructures Initiative. We are grateful to S. Lizzit and A. Baraldi for their contribution.

■ REFERENCES

(1) Nørskov, J. K.; Abild-Pedersen, F. *Nature* **2009**, *461*, 1223−5.
(2) Loffreda, D.; Delbecq, F.; Vigné, F.; Sautet, P. *Angew. Chem., Int. Ed.* **2009**, *48*, 8978−80.
(3) Gan, L.; Tian, R.; Yang, X.; Lu, H.; Zhao, Y. *J. Phys. Chem. C* **2012**, *116*, 745−752.
(4) Rizzi, M.; Furlan, S.; Peressi, M.; Baldereschi, A.; Dri, C.; Peronio, A.; Africh, C.; Lacovig, P.; Vesselli, E.; Comelli, G. *J. Am. Chem. Soc.* **2012**, *134*, 16827−33.
(5) Grabow, L. C.; Hvolbæk, B.; Nørskov, J. K. *Top. Catal.* **2010**, *53*, 298−310.
(6) Nerlov, J.; Chorkendorff, I. *Catal. Lett.* **1998**, *54*, 171−176.
(7) Nerlov, J.; Chorkendorff, I. *J. Catal.* **1999**, *181*, 271−279.
(8) Peterson, A. A.; Nørskov, J. K. *J. Phys. Chem. Lett.* **2012**, *3*, 251−258.
(9) Behrens, M.; Studt, F.; Kasatkin, I.; Kühl, S.; Hävecker, M.; Abild-Pedersen, F.; Zander, S.; Girgsdies, F.; Kurr, P.; Kniep, B.-L.; Tovar, M.; Fischer, R. W.; Nørskov, J. K.; Schlögl, R. *Science (New York, N.Y.)* **2012**, *336*, 893−7.
(10) Dri, C.; Peronio, A.; Vesselli, E.; Africh, C.; Rizzi, M.; Baldereschi, A.; Peressi, M.; Comelli, G. *Phys. Rev. B* **2010**, *82*, 1−6.
(11) Ding, X.; De Rogatis, L.; Vesselli, E.; Baraldi, A.; Comelli, G.; Rosei, R.; Savio, L.; Vattuone, L.; Rocca, M.; Fornasiero, P.; Ancilotto, F.; Baldereschi, A.; Peressi, M. *Phys. Rev. B* **2007**, *76*, 195425.
(12) Vesselli, E.; Rizzi, M.; De Rogatis, L.; Ding, X.; Baraldi, A.; Comelli, G.; Savio, L.; Vattuone, L.; Rocca, M.; Fornasiero, P.; Baldereschi, A.; Peressi, M. *J. Phys. Chem. Lett.* **2010**, *1*, 402−406.
(13) Vesselli, E.; De Rogatis, L.; Ding, X.; Baraldi, A.; Savio, L.; Vattuone, L.; Rocca, M.; Fornasiero, P.; Peressi, M.; Baldereschi, A.; Rosei, R.; Comelli, G. *J. Am. Chem. Soc.* **2008**, *130*, 11417−22.
(14) Vesselli, E.; Schweicher, J.; Bundhoo, A.; Frennet, A.; Kruse, N. *J. Phys. Chem. C* **2011**, *115*, 1255−1260.
(15) Ernst, K.-H.; Schlatterbeck, D.; Christmann, K. *Phys. Chem. Chem. Phys.* **1999**, *1*, 4105−4112.
(16) Demirci, E.; Carbogno, C.; Groß, A.; Winkler, A. *Phys. Rev. B* **2009**, *80*, 085421.
(17) Baraldi, A.; Comelli, G.; Lizzit, S.; Cocco, D.; Paolucci, G.; Rosei, R. *Surf. Sci.* **1996**, *367*, L67−L72.
(18) Briner, B. G. *Science* **1997**, *278*, 257−260.
(19) Studt, F.; Abild-Pedersen, F.; Wu, Q.; Jensen, A. D.; Temel, B.; Grunwaldt, J.-D.; Nørskov, J. K. *J. Catal.* **2012**, *293*, 51−60.
(20) Nerlov, J.; Sckerl, S.; Wambach, J.; Chorkendorff, I. *Appl. Catal., A* **2000**, *191*, 97−109.
(21) Knop-Gericke, A.; Kleimenov, E.; Havecker, M.; Blume, R.; Teschner, D.; Zafeiratos, S.; Schlögl, R.; Bukhtiyarov, V.; Kaichev, V. V.; Prosvirin, I. P.; Nizovskii, A.; Bluhm, H.; Barinov, A.; Dudin, P.; Kiskinova, M. *Adv. Catal.* **2009**, *52*, 213−272.
(22) Rupprechter, G. *MRS Bull.* **2007**, *32*, 1031−1037.
(23) Grabow, L. C.; Mavrikakis, M. *ACS Catal.* **2011**, *1*, 365−384.
(24) Liu, C.; Cundari, T. R.; Wilson, A. K. *J. Phys. Chem. C* **2012**, *116*, 5681−5688.
(25) Liem, S. Y.; Clarke, J. H. R. *J. Chem. Phys.* **2004**, *121*, 4339−45.